



Drought monitoring in Croatia using the standardized precipitation-evapotranspiration index

Ivan Lončar-Petrinjak ¹, Zoran Pasarić ² and Ksenija Cindrić Kalin ¹

¹ Croatian Meteorological and Hydrological Service, Zagreb, Croatia

² Department of Geophysics, Faculty of Science, University of Zagreb, Zagreb, Croatia

Received 29 December 2023, in final form 27 May 2024

Several periods of drought in the 21st century have severely affected large parts of Europe and caused considerable economic losses, particularly in the agricultural and energy sectors. While rainfall deficits are one of the main causes of droughts, high temperatures in the summer months exacerbate their development, which can have devastating consequences. This was the case in 2022, when long dry spells were accompanied by several heat waves. In this study, climatological drought monitoring using the Standardized Precipitation Evapotranspiration Index (*SPEI*) is analyzed with the primary goal of finding the best theoretical distribution for adjusting the water balance (defined as the difference between precipitation and potential evapotranspiration) in Croatia before the index is officially introduced into the operational drought monitoring. Although the *SPEI* is widely used for drought monitoring, the underlying theoretical distribution of the water balance may differ between regions. The study is based on monthly precipitation amounts and monthly mean values of daily minimum and maximum temperatures observed at 31 main meteorological stations for the period 1961–2022. The analysis is carried out for different time scales, ranging from 1 to 24 months. Among the five distributions considered, a generalized logistic distribution with three parameters (GLO) proves to be the most appropriate. There is general agreement between *SPEI* and *SPI* time series, both in terms of sign and intensity. However, in periods with a light to moderate lack of precipitation and high air temperatures, a tendency towards higher drought intensity prevails in the *SPEI*. A comparative analysis of the 2022 drought in Croatia confirmed the ability of the *SPEI* to detect a drought earlier than the *SPI*, which also suggests that a larger area of the country was affected by the drought due to consistent air temperature excesses.

Keywords: drought, precipitation, air temperature, *SPI*, *SPEI*, generalized logistic distribution, L-moments

1. Introduction

Drought is a natural phenomenon caused by a lack of water, primarily due to a lack of rainfall, although evapotranspiration is also an important variable

in the persistence of drought (Lloyd-Hughes and Saunders, 2002). It manifests itself in dry weather and below-normal moisture levels in the ecosystem, which inhibits plant growth and disrupts phenological stages due to the lack of water. Prolonged drought can reduce or completely ruin crop yields, especially when combined with heat stress caused by high air temperatures, resulting in significant socio-economic damage. In the 21st century, large parts of Europe have so far been hit by several droughts (Blauhut et al. 2022 and references therein), causing high economic losses, especially in the agriculture and energy sectors. In Croatia, the 2011/2012 drought was the most devastating drought that affected the entire country (Cindrić et al., 2016). It was caused by two intense blocking episodes over Central Europe, which prevented cold and humid air from the north from bringing precipitation to the area. It has been shown that the main reason for the prolonged drought was the lack of precipitation and, to a lesser extent, the high air temperature. However, the recent drought in 2022, which was accompanied by several heat waves in summer, has devastated the agricultural production in large parts of Croatia, but also in large parts of Europe. Schumacher et al. (2023) analyzed the European drought of 2022 in terms of summer soil moisture using both observations and climate models. Their results showed that excessive heat and lack of precipitation probably played an important role in the occurrence of the summer drought. The lack of water supply lasted long enough to lead to a hydrological drought, resulting in groundwater depletion, falling water levels in lakes, rivers and other reservoirs.

There are many indices in the literature to describe drought in a climatological context, and the most used are the Standardized Precipitation Index (SPI), the Standardized Precipitation-*evapotranspiration* Index (SPEI), the self-calibrating Palmer Drought Severity Index (sc-PDSI), the China Z-index (CZI) and the Rainfall Decile based Drought Index (RDDI) (Zargar et al., 2011). In climatological practice, however, the SPI is most commonly used for operational drought monitoring due to the recommendation of the World Meteorological Organization (WMO) (Svoboda et al., 2012). The SPI is easy to calculate because it depends only on the amount of precipitation and can be applied on any time scale. However, the SPEI has been increasingly used recently as it is not only used to monitor the precipitation deficit but also the water balance (by including *evapotranspiration* estimates) and is still simple enough to be used operationally.

Syed et al. (2008) showed that precipitation is the most important factor for groundwater reserves in the tropics, while *evapotranspiration* is more important for describing the variability of the water balance in the mid-latitudes. It is known that *evapotranspiration* increases with increasing air temperature, as warmer air removes more moisture from the surface. In this context, Vicente-Serrano et al. (2010) investigated the performance of SPEI compared to SPI and sc-PDSI at eleven stations in different climate zones worldwide. They recommended the log-logistic theoretical distribution for fitting water balance values as the most appropriate for different climate regimes around the globe. They

tested the ability of SPEI to detect dry spells and evaluated their duration and intensity on different time scales. The time series of SPI, sc-PDSI and SPEI on different time scales were compared under the two scenarios for the increase in global air temperature. In a scenario without temperature increase, the sc-PDSI and SPEI did not differ significantly from the SPI, but with increasing temperatures, these two indices reacted earlier to mark the onset of dry spells and showed an increase in the intensity of dry spells. This finding was true for all stations and time scales considered. In addition, Vicente-Serrano et al. (2014) demonstrated that rising surface air temperatures lead to longer and more intense dry spells.

The drought indices for Croatia have already been examined in various studies. The pioneering work was done by Penzar (1976), who analyzed the characteristics of drought using the Palmer Drought Severity Index (PDSI) on the basis of long-term data from the Zagreb-Maksimir station. Subsequently, Pandžić (1985) used the same Palmer model to investigate the water balance characteristics at different soil depths throughout the Adriatic region and found spatial and temporal differences in soil saturation. Subsequent studies found temporal changes in the water balance, as evidenced by positive trends in potential evapotranspiration (Vučetić and Vučetić, 1994, 1996a, 1996b; Gajić-Čapka and Zaninović, 1998). In addition, Pandžić et al. (2009) demonstrated a strong correlation between negative trends in long-term fluctuations in soil moisture and global warming. Mihajlović (2006) used the Standardized Precipitation Index (SPI) to analyze the 2003–2004 drought in the Pannonian region of Croatia and confirmed that the SPI is a valuable tool for operational drought monitoring. In a comparative study, Pandžić et al. (2020) evaluated the PDSI and the Standardized Precipitation Index (SPI) at the Zagreb-Grič station and concluded that the PDSI more clearly highlights the long-term drought/wetness variations. More recently, Pandžić et al. (2022) found that the self-calibrating PDSI has a better correlation with drought-affected maize yield than the SPI on comparable time scales. However, due to its high autocorrelation, the PDSI is less suitable for capturing short-term fluctuations that are crucial for operational drought monitoring.

Given rising global air temperatures and clear future scenarios for a warmer climate (Allan et al., 2021), it seems reasonable to use a heat-sensitive drought index to better describe the quantitative nature of dry spells in operational drought monitoring (ODM). At the Croatian Meteorological and Hydrological Service (DHMZ), the SPI is commonly used for ODM, with its calculation based on a gamma distribution. However, when the absence of precipitation is accompanied by extreme air temperatures, especially in the summer months, the SPI may not be sufficient to realistically monitor the intensity and extent of drought. Therefore, the main motivation for this study was to analyze the utility of the SPEI for operational drought monitoring in the DHMZ. Although the SPEI is widely used for drought monitoring and the recommended log-logistic distribu-

tion is commonly used to ensure comparability, the underlying theoretical distribution for the water balance may differ across regions. Although Croatia is a rather small country, it is nevertheless a very diverse country spanning different climate zones. Therefore, it is important to test different distributions before introducing a national drought monitoring product. A similar procedure was carried out when the SPI for Croatia was analyzed (Cindrić et al., 2019). Therefore, the main objectives of this study are i) to find the best fitting statistical distribution for the water balance (defined as the difference between precipitation and evapotranspiration) in Croatia as the main variable for SPEI calculation and ii) to compare the results of SPI and SPEI for a specific event in Croatia such as the recent drought in 2022 in terms of duration, intensity and extent. The authors believe that the new drought monitoring index, available to end-users and stakeholders, will be useful in improving drought management in Croatia.

2. Data and methods

The data used in this study comprise the monthly precipitation totals and the monthly mean values of the daily minima and maxima of air temperature at 31 main meteorological stations from the DHMZ station network (Fig. 1). The set of stations, which is divided into seven regions characterized by precipitation regimes and defined by Gajić-Čapka et al. (2015), is used by the DHMZ for real-time drought monitoring (www.meteo.hr). The data used here covered the common measurement period 1961–2022.

The standardized indices *SPI* and *SPEI* are numerical indicators of the dryness or wetness of a region on a specific time scale. The *SPI* considers only the absence or excess of precipitation (*P*) during a given period (McKee et al., 1993). The *SPEI* requires at least two input variables – in addition to precipitation, other climate parameters should be available, depending on the method chosen to calculate potential evapotranspiration (*PET*), which is then subtracted from precipitation to obtain the measure of water balance, $D = P - PET$ (Vicente-Serrano et al., 2010). In the present study, a simple modified Hargreaves-Samani formula was used to calculate the monthly *PET* (Droogers and Allen, 2002), which only takes into account the mean maximum and minimum monthly air temperature values:

$$PET = 0.0013 \cdot 0.408 R_a \cdot (T + 17.8) \cdot (T_{max} - T_{min} - 0.0123P)^{0.76}. \quad (1)$$

Here 0.0013 and 0.0123 are the coefficients of the modified Hargreaves method, R_a is the extraterrestrial solar radiation in *mm/day* and the constant 0.408 is used to convert the radiation into evaporation equivalents in mm. T_{min} and T_{max} are the monthly mean values of the minimum and maximum daily temperatures respectively, $T = (T_{min} + T_{max}) / 2$, while *P* is the monthly precipitation in *mm/month*.

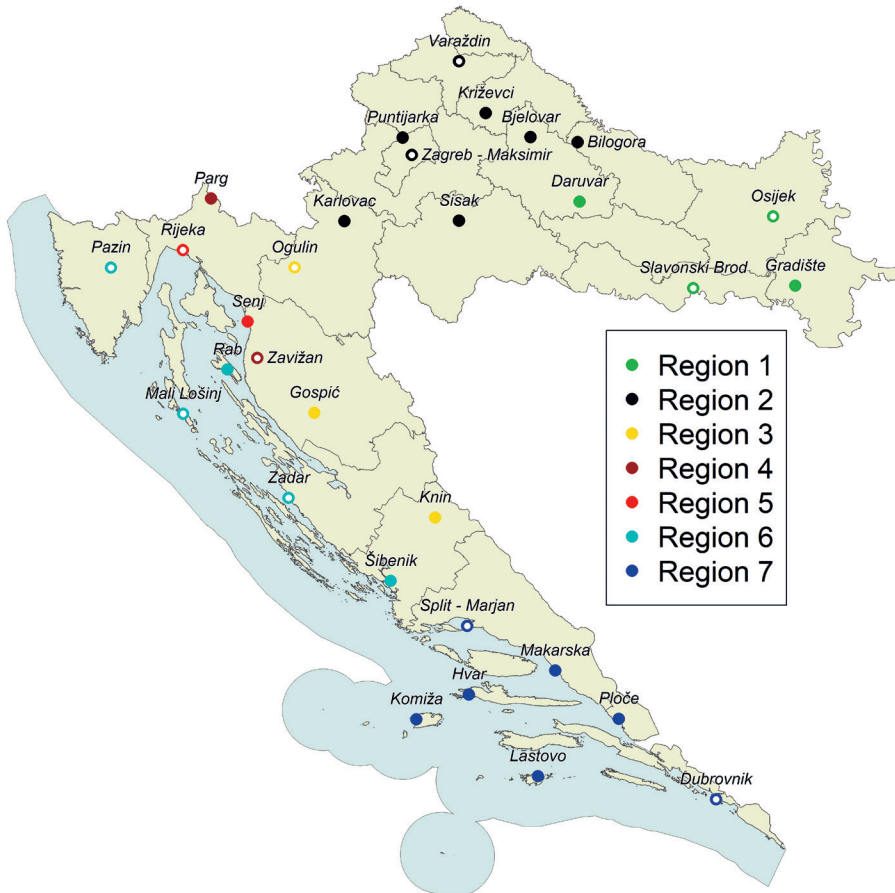


Figure 1. Geographical location of the 31 meteorological stations in Croatia used in this study. Seven regions (1 – eastern mainland, 2 – western mainland, 3 – central hinterland, 4 – mountainous, 5 – mountainous littoral, 6 – northern Adriatic coastal and 7 – central and southern Adriatic) are indicated by corresponding colors. Empty symbols indicate stations that will be referred to later (see Fig. 9).

The use of a small number of variables for PET estimation is advantageous in operational drought monitoring, and although the method is simple, it provides more reliable results than the Thornthwaite method (Amatya et al., 1995). The R package “SPEI” has been used for both SPI and $SPEI$ estimations (Beguiria and Vicente-Serrano, 2022).

The methods for calculating the two indices are similar, the only difference being the underlying theoretical distributions of P and D for SPI and $SPEI$ respectively. For the calculation of the SPI , a gamma distribution is usually chosen to fit the empirical frequency distribution of precipitation totals on different time

scales (usually for 1, 2, 3, 6, 9, 12, 18 and 24 months). Cindrić et al. (2019) confirmed the gamma distribution as suitable for precipitation monitoring in Croatia. The obtained cumulative probabilities are then transformed into the standard normal distribution (mean equal to zero and standard deviation equal to one), resulting in the respective *SPI* values. The procedure for the *SPEI* calculation is the same, but with a different underlying theoretical distribution. It must be a three-parameter distribution that considers both negative and positive values of the water balance variable. Vicente-Serrano et al. (2010) tested the following set of candidate distributions: Pearson type III, generalized extreme value distribution, log-logistic distribution (within the generalized logistic distribution), generalized Pareto distribution, and log-normal distribution (as a member of the generalized normal distribution family). The cumulative distribution functions of these distributions are as follows:

Pearson type III distribution (PE3):

$$F(x) = G\left(\alpha, \frac{x - \xi}{\beta}\right) / \Gamma(\alpha), \quad (2)$$

where $G(\alpha, x) = \int_0^x t^{\alpha-1} e^{-t} dt$ and $\Gamma(\cdot)$ is the gamma function.

Generalized Extreme Value distribution (GEV):

$$F(x) = e^{-e^{-y}}. \quad (3)$$

Generalized Logistic distribution (GLO):

$$F(x) = 1/(1 + e^{-y}). \quad (4)$$

Generalized Pareto distribution (GPA):

$$F(x) = 1 - e^{-y}. \quad (5)$$

Generalized Normal distribution (GNO):

$$F(x) = \Phi(y). \quad (6)$$

Here Φ is the cumulative distribution function of the standard normal distribution, and

$$y = -k^{-1} \log\{1 - k(x - \xi)/\alpha\}, \text{ for } k \neq 0,$$

$$y = (x - \xi)/\alpha, \text{ for } k = 0,$$

for GEV, GLO, GPA and GNO distributions.

We also considered the same pool of distributions for the Croatian data. To estimate the parameters of the distributions, we used the method of L-moments (Hosking and Wallis, 1997), which is more robust to data outliers in small sam-

ples than the maximum likelihood method. The L-moments are linear combinations of the probability weighted moments (PWMs). We used the R package “*lmom*” version 2.9 (Hosking, 2022) to fit the distributions. To avoid possible confusion regarding the terminology used in the literature and software, it should be noted here that the GLO distribution of Hosking and Wallis (1997) is a reparametrized version of the log-logistic distribution commonly used as a candidate distribution for *SPEI* calculation (Vicente-Serrano et al., 2010). Similarly, the GNO distribution (named as such in the R package “*lmom*”, but not in Hosking and Wallis, 1997) is a reparametrized version of the log-normal distribution. The distributions in the R package and in the book are the same, only their names are different in the case of the log-normal distribution. For consistency, these two distributions are referred to here as the log-logistic and log-normal distributions but abbreviated as GLO and GNO respectively.

The choice of a distribution that best fits the water balance D was carried out in several steps. First, the L-moment ratios of the empirical water balance data for all candidate distributions were plotted in the L-moment ratio diagram. Distributions that deviated significantly from the main group of empirical points were discarded. The remaining distributions were further tested using the Kolmogorov-Smirnov (*KS*) statistical test (Wilks, 2011), which compares the empirical and theoretical (fitted) cumulative distribution functions. More specifically, the *KS* statistic (denoted KS_n) is a measure of goodness of fit, defined as the maximum difference between an empirical ($F_n(x)$) and a theoretical distribution function ($F(x)$):

$$KS_n = \max_x |F_n(x) - F(x)|. \quad (6)$$

Under the null hypothesis that the sample originates from the theoretical distribution, the statistic for n , which is sufficiently large, approximates the so-called Kolmogorov distribution, regardless of what the true underlying distribution looks like (Wilks, 2011). However, when the distribution parameters are calculated from data, there is some bias that cannot be ignored. In this case, the proposed theoretical distribution is more inclined to successfully fit the data (Crutcher, 1975). To overcome this problem and reduce the probability of a type II error, the Lilliefors test was performed using Monte Carlo simulations (Blain, 2014). For each candidate distribution, the procedure is as follows: For each combination of station, month and time scale (SMT), the L-moments were calculated, and the corresponding distribution parameters were determined. Then, using the obtained parameters, 1000 samples with a size of 60 (corresponding to the original data sample length) were simulated, and the *KS* test procedure was performed for each simulated data set. The resulting 1000 *KS* statistic values approximate the test statistic distribution, from which the 95th percentile was extracted as the critical value and then used to perform the *KS* test for a given combination of SMT.

3. Results

3.1. The choice of theoretical distribution for SPEI

First, the five theoretical distributions with the corresponding pdfs described by Eqs. (1)–(5) are tested for the adjustment of the water balance in Croatia. The L-moment ratio diagrams for all stations and selected time scales (1, 3, 6 and 12 months) are shown in Fig. 2 (a–d). The empirical L-skewness and L-kurtosis are depicted with dots together with the theoretical curves for five considered distributions. Each dot corresponds to a particular station, with the color indicating the respective region (see Fig. 1), and for each station there are 12 dots, one for each month of a year. It can be seen that the empirical L-moment ratios (dots) generally tend to cluster together, and that the “cloud” is slightly shifted towards the L-skewness value of zero as the time scale increases. This could be a consequence of the decreasing variability of the water balance with increasing time scale. Another noticeable feature is the grouping of dots representing the same region, especially on larger time scales.

For example, on a time scale of 12 months, the green dots representing region 1 (eastern mainland) group around the skewness of about -0.04 and a kurtosis of 0.14. The slightly negative skewness on the annual scale indicates more fre-

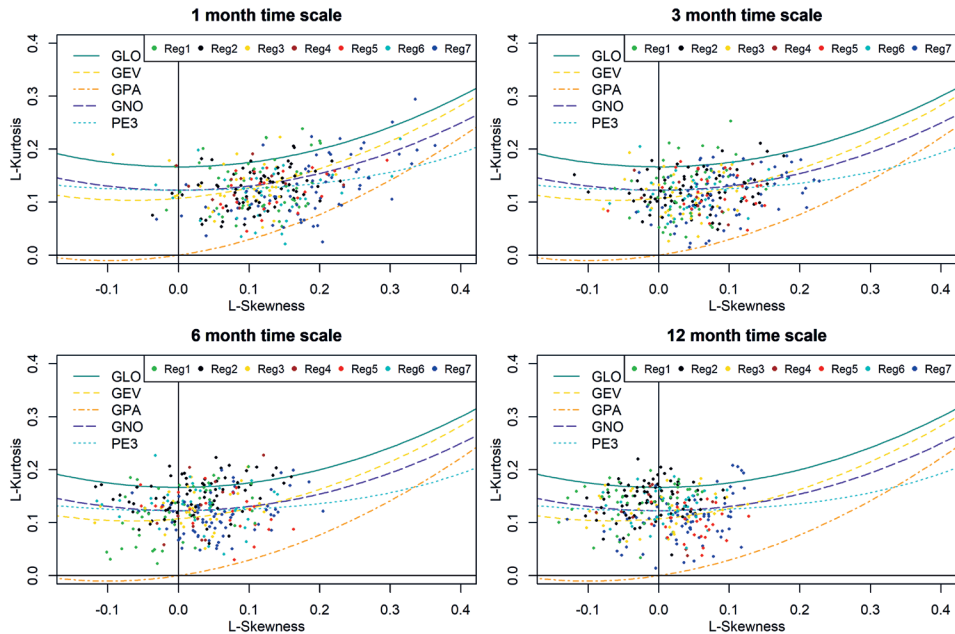


Figure 2. L-moment ratio diagrams for a) 1-, b) 3-, c) 6- and d) 12-month time scales. The dots represent empirical L-moment ratios for each of the 12 months of a year for each station. The lines represent the L-moment ratios for five theoretical distributions. The stations are grouped into 7 regions indicated by different colors (see Fig. 1).

quent dry periods than wet periods. In southern Croatia (Central and southern Adriatic, Reg7, represented by blue dots), the dots grouped around a skewness of 0.05 and a kurtosis of 0.1. This distribution is slightly skewed to the right, resulting in a slightly longer right tail of the distribution. In comparison to region 1, wet events occur more frequently than dry events. Such a grouping is therefore an expression of regional climate characteristics.

At first glance, it is clear from the L-moment ratio diagrams that the generalized Pareto distribution (GPA) does not represent the water balance data well and that the curve of the generalized logistic distribution (GLO) also deviates from the majority of empirical points. The empirical L-moment ratios oscillate around the remaining candidate distributions. The goodness of fit of the five distributions was further tested using the KS test according to the procedure described in Section 2. Table 1 summarizes the results for all stations and months for different time scales. The percentage of cases that passed the KS test for the five theoretical distributions is shown. It can be seen that the null hypothesis that the sample originates from each of the theoretical distributions tested cannot be rejected. However, the lowest percentage is found for the generalized Pareto distribution, which is consistent with the results shown in Fig. 2. Overall, the highest percentage of *PET* cases followed the GLO distribution in all time scales analyzed, while the second and third best options were the PE3 and GEV distributions, respectively. Table 2 shows the best fitting distribution for all stations for each month and time scale. When multiple distributions perform equally well, the GLO distribution is preferred (in text and color) based on the results from Tab. 1, and the number of remaining equally well-fitting distributions is indicated by the number of “x” symbols. It was found that for some months and time scales (e.g. August, time scales of 1 and 6 months), other three distributions besides the GLO can be used for fitting the *PET* in Croatia. Considering these results and taking into account that the GLO distribution was also recommended by Vicente-Serrano et al. (2010), we chose the GLO distribution as the best option for practical applications.

Table 1. Percentage of cases in which the calculated KS statistic associated with different theoretical distributions (Distr.) falls below the critical KS value (meaning that the null hypothesis is not rejected) for all stations and months.

Distr.	Time scale [months]							
	1	2	3	6	9	12	18	24
GNO	89.2	88.4	84.7	90.3	92.2	89.2	89.8	89.0
GLO	96.0	96.2	97.6	95.7	97.3	96.0	96.5	94.4
PE3	94.4	95.2	95.7	95.7	96.2	95.4	94.4	93.3
GEV	94.4	94.9	94.9	94.4	94.9	94.4	93.3	91.1
GPA	72.0	63.2	57.3	43.3	37.4	41.9	45.7	42.7

Table 2. Best-fit distributions for the water balance across all stations. When the percentage of non-rejected null hypotheses is the same for multiple distributions, the GLO distribution is preferred in text and color, and the number of remaining equally well-fitting distributions is indicated by the number of "x" symbols. The cells are colored according to the color codes contained in Tab. 1.

Month	Time scale [months]							
	1	2	3	6	9	12	18	24
Jan	GLOx	GLOxx	GLOx	GNO	GLOxx	GLOx	GLOx	GLO
Feb	GLOx	GLOx	GLO	GLOxx	GLOxx	GLOxx	GLOx	GLO
Mar	GLOxx	GLOxx	GLOx	GLOx	GLO	GLOx	GLO	GLOx
Apr	GLOxx	GNO	GLO	GLOxx	GLOxx	GLOxx	GLOxx	GEV
May	GLO	GLO	GNO	GLOxx	GLO	GLO	GLOxx	GNO
Jun	GEV	GNO	GLO	GLOxx	GLO	GLOxx	GLO	GNO
Jul	GLO	GNO	GLOx	GLOxxx	GLOxx	GNO	GLO	GNO
Aug	GLOxxx	GLOx	GLOx	GLOxxx	GLO	GNO	GLOxx	GLOx
Sep	GLOx	GLOx	GLOx	GLOx	GLOxxx	GLOxxx	GLO	GLOxx
Oct	GLO	GLOxx	GLOx	GLOx	GLOxxx	GLOxx	GLOx	GLOxxx
Nov	PE3	GLO	GLOxx	GLOx	GLOxx	GLOxxx	GLO	PE3
Dec	GLOxx	GLOxx	GLO	GLOxx	GLOxx	GLO	GLOxx	GLO

As an example of the analysis of the monthly water balance, Figs. 3 and 4 show the L-moment ratio diagram for the Zagreb-Maksimir station and the fitted GLO distribution on a monthly scale. There is a reasonable correspondence be-

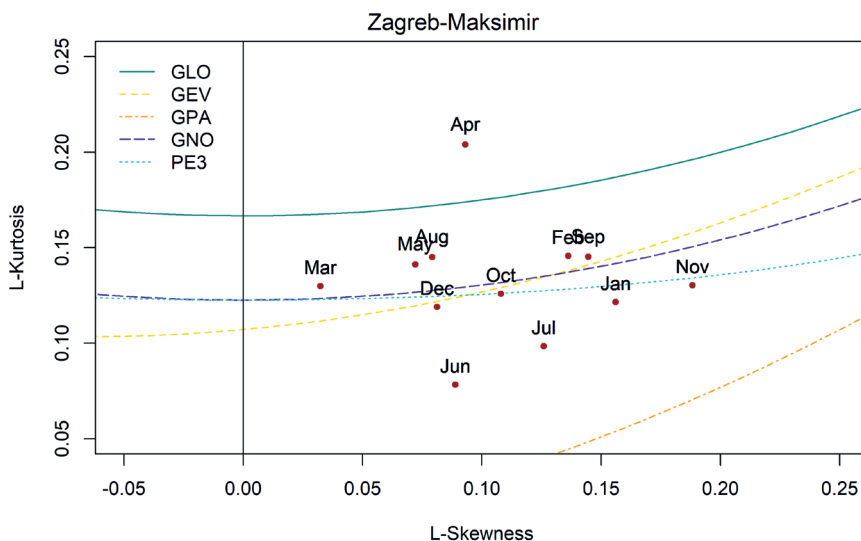


Figure 3. Empirical (dots) and theoretical (curves) L-moment ratios for each month of the year for the Zagreb-Maksimir station.

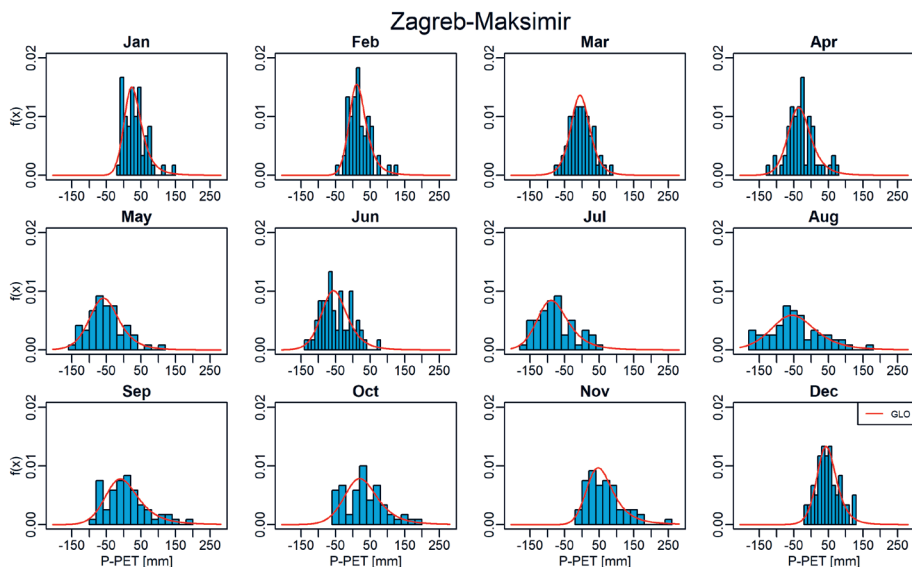


Figure 4. Histograms of the water balance (*blue*) and fitted log-logistic distribution (GLO) (*red line*) for each month in a year for the Zagreb-Maksimir station.

tween the L-moment ratio diagram and the shape of the fitted distribution. All distributions are positively skewed, with the distribution being most skewed in November and least skewed in March. This can be interpreted to mean that heavy precipitation (high water balance values) occurs in a less consistent manner in November, and such events are considered extremes. On the other hand, the distribution in March appears more symmetrical. April has the highest value of kurtosis, while June has the lowest. If only the kurtosis is considered, this would indicate that the April precipitation has a somewhat heavier tails, thus large amounts of precipitation are recorded more frequently. In June, on the other hand, a lower kurtosis indicates shorter tails and thus a smaller number of large events.

3.2. Comparison of drought analysis based on SPI and SPEI

Figure 5(a-d) shows the time series of *SPI* and *SPEI* on time scales of 1, 3, 6 and 12 months for the stations Gospić, Osijek, Split-Marjan and Zagreb-Maksimir. The reference period for calculating the parameters of the gamma and GLO distributions was 1961–2020.

The results show that the *SPEI* follows the *SPI* on all time scales, as one would expect. Changes between positive and negative values occur on time scales that roughly correspond to the respective index time scale. On shorter scales, positive and negative values oscillate with a period of one to three months, while

on longer time scales (12 months) oscillations occur with periods of one to several years. After the 1990s, the magnitude and duration of wet and dry spells increased on longer time scales in the continental regions (Fig. 5a, b); the corresponding magnitudes also increased in the mountainous region (Fig. 5c), and the frequency of oscillations increased on the coast (Fig. 5d), with more intense dry spells, especially since 2015. In general, *SPEI* values are lower in warm periods and higher in cold periods, which is to be expected due to the impact of air temperature on the potential evapotranspiration used for *SPEI* calculation. In cold months with monthly temperatures around the freezing point, evapotranspiration is low and the water balance is close to the amount of precipitation, which is then perceived as moisture excess. Thus, the *PET* can be considered as a correction factor, while precipitation deficit (surplus) is still considered the main trigger for dry (wet) periods. For this reason, *SPEI* tends to show lower values (more intense drought) than *SPI* during dry periods when *SPI* is approximately between 0 and -1.5 and higher values when *SPI* is below -1.5 . In the first 20 years of the period studied (up to the 1980s), both indices show more wet than dry periods, followed by a long dry period in the first half of the 1990s and a wet period in the second half of the decade. In the 21st century, greater fluctuations between extremely wet and dry periods with more pronounced

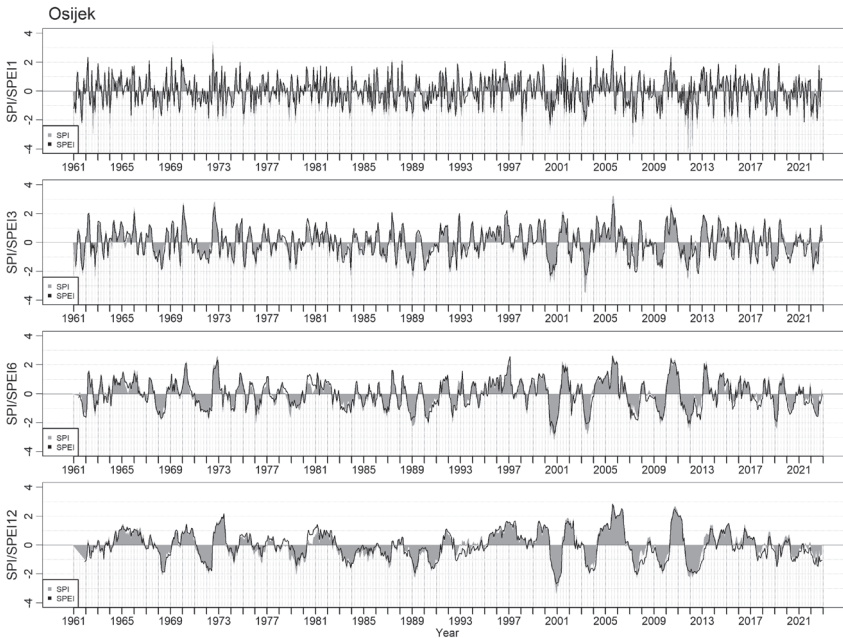


Figure 5 a). *SPI* and *SPEI* time series for the Osijek station in the period 1961–2022. The shaded area shows the *SPI* and the black lines the *SPEI* values.

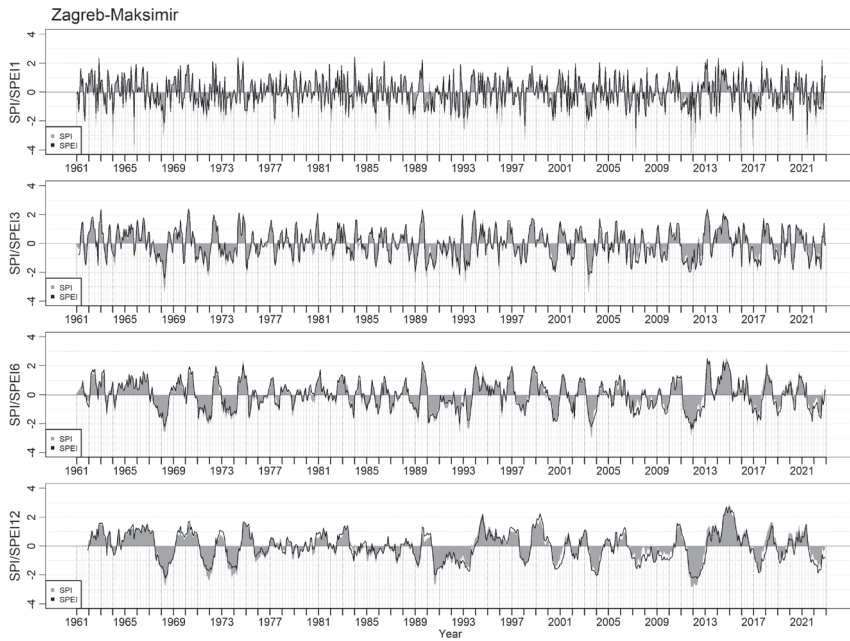


Figure 5 b). The same as in Fig. 5a, but for the station Zagreb-Maksimir.

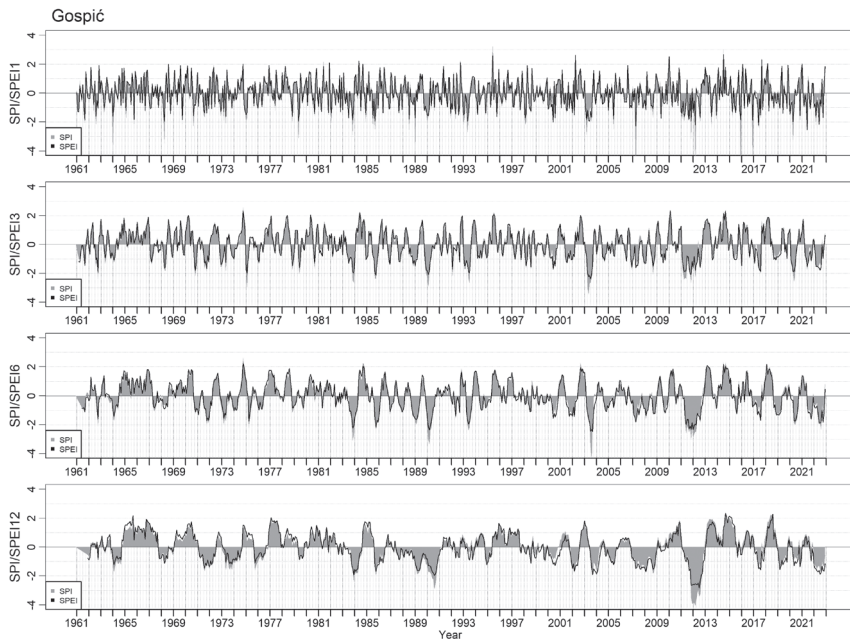


Figure 5 c). The same as in Fig. 5a, but for the Gospić station.

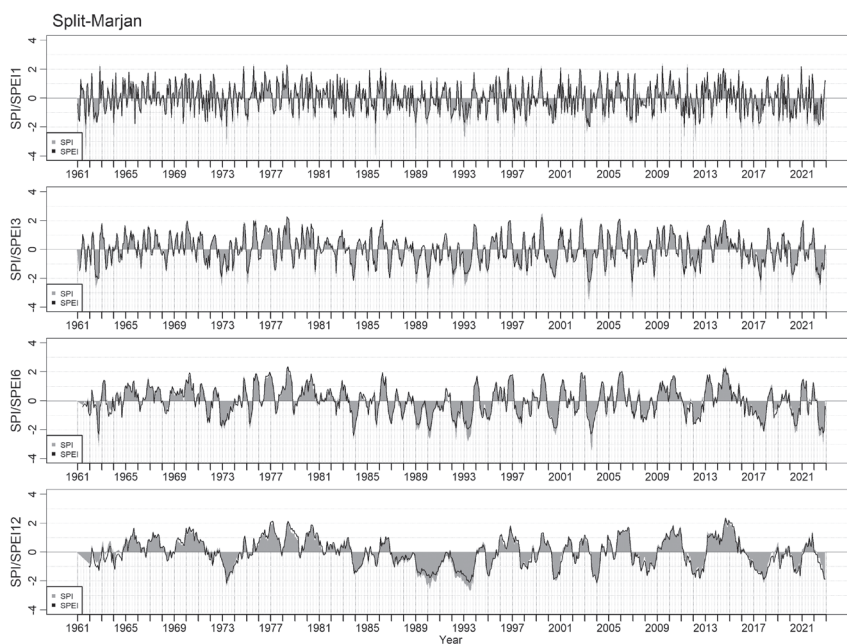


Figure 5 d). The same as in Fig. 5a, but for the Split-Marjan station.

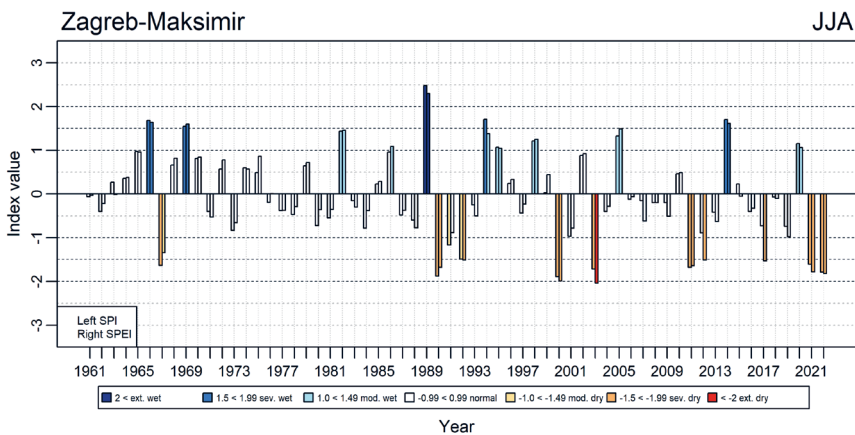


Figure 6. Comparison of *SPI* (left bars) and *SPEI* (right bars) for the summer season (3-month time scale for August) in the period 1961–2022 at the Zagreb-Maksimir station.

droughts were observed throughout Croatia, especially during the last decade in the mountainous and coastal regions.

The seasonal comparison of summer *SPI* and *SPEI* (3-month time scale for August) is shown in Fig. 6 for the Zagreb-Maksimir station. The different catego-

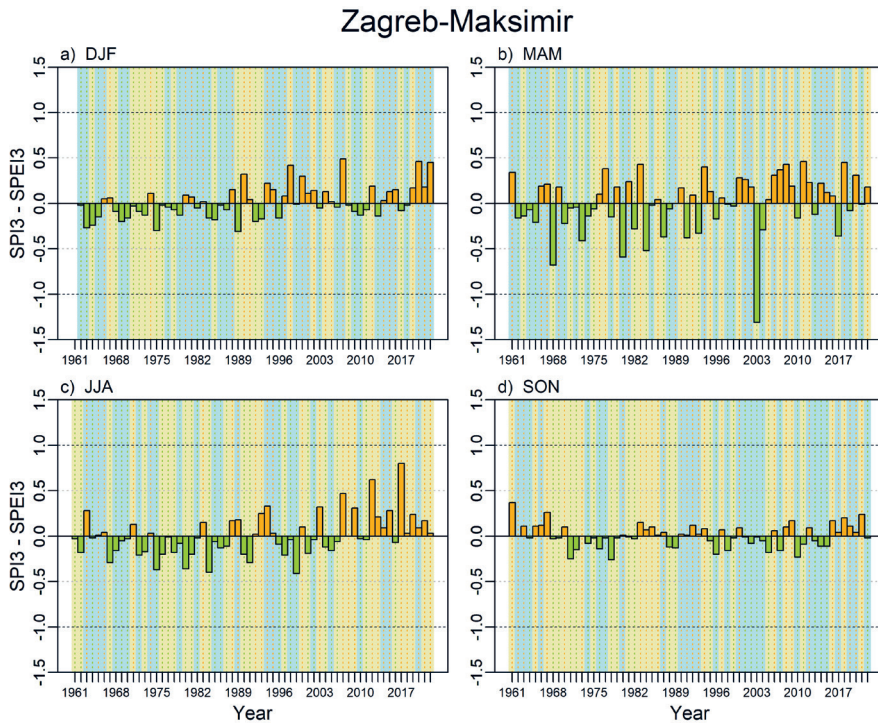


Figure 7. Differences between *SPI3* and *SPEI3* for a) DJF, b) MAM, c) JJA and d) SON during the period 1961–2022 at the Zagreb-Maksimir station. Blue (golden) shading of the background indicates wet (dry) periods.

ries of dry and wet conditions are marked with red and blue shades. In the second half of the analyzed period, there were significantly more dry summers with seven (nine) dry summers since the 1990s according to the SPI (SPEI), while there was only one in the previous period. Since the 2000s, the SPEI has shown lower values than the SPI for most dry summers.

The seasonal differences between the two indices, SPI-SPEI, show a trend towards more dryness and less wetness in all seasons, with pronounced trends in spring and summer (Fig. 7). Positive trends in the difference between SPI and SPEI values are more pronounced in the warm half of the year (April–September), which generally corresponds to the growing season in Croatia, than in the cold half of the year (October–March) (not shown). These results can be attributed to the significant warming trend in Croatia in spring and summer (UNFCCC, 2023, https://unfccc.int/sites/default/files/resource/NC8_BR5_HR_resubmission.pdf).

The largest differences between SPI and SPEI at the Zagreb-Maksimir station were observed during the spring 2003 drought (Fig. 7b), suggesting that it

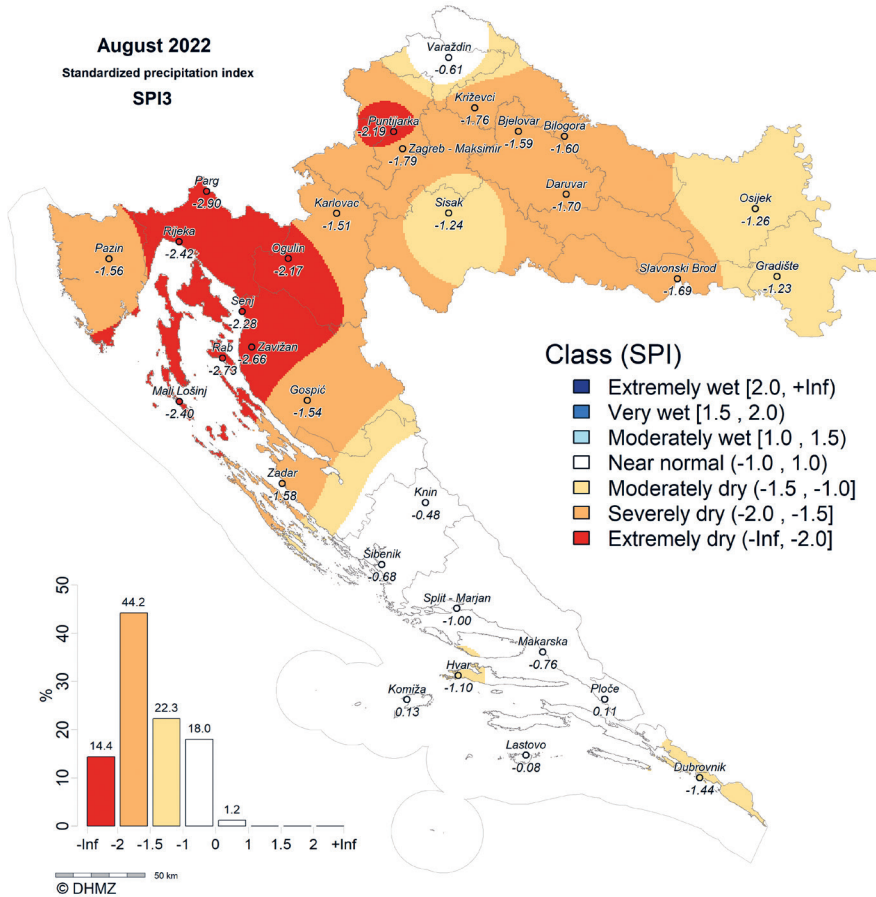


Figure 8 a). SPI for summer of 2022.

was primarily caused by the precipitation deficit, while the summer excess of air temperature contributed to the effectiveness of the drought and resulted in larger negative values for *SPEI* compared to *SPI* (Fig. 7c). To show the effect of temperature in more detail, the 2022 drought was further analyzed, as positive anomalies of mean monthly air temperatures prevailed in Croatia from March to November, especially during JJA and SON (not shown). The spatial distributions of the two representative three-month *SPI* and *SPEI* for summer 2022 in Croatia are shown in Fig. 8 (a, b). The spatial interpolation was performed using the inverse distance method.

Overall, the *SPEI* shows a larger area affected by drought than the *SPI*, with the biggest difference being in the severe drought class, which rises from 44.2% to 67% of the total area. In this context, there is a significant decrease in near-normal conditions to only 2%, but the extremely dry area has also decreased (by

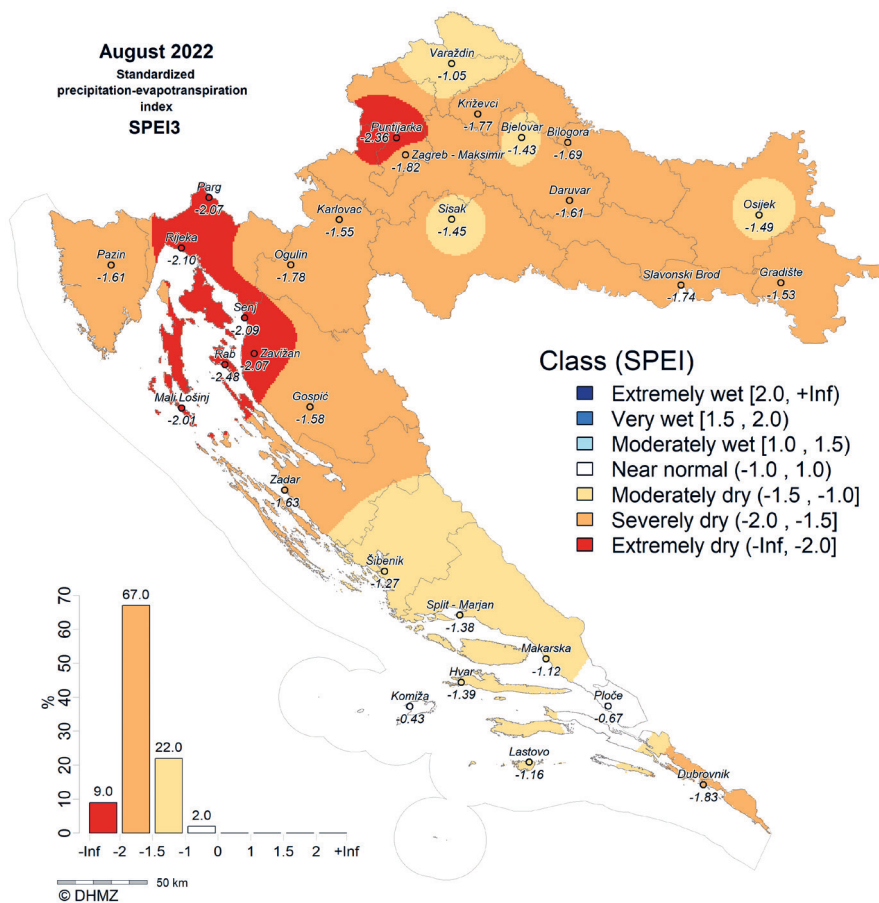


Figure 8 b). SPEI for summer of 2022.

5.3% compared to the *SPI*). This corresponds to the fact that the *SPEI* reacts most strongly to the air temperature when the dryness according to the *SPI* is approximately between -1.5 and 1.5 . This shows that precipitation gives more weight to the index and air temperature is taken into account as a correction factor. For example, 155 mm of precipitation was measured at the Ogulin station in the three-month period, compared to only 43 mm in Dubrovnik. Nevertheless, Ogulin was classified as extremely dry ($SPEI3 = -2.17$) based on the shape of the respective probability distributions, while Dubrovnik was classified as moderately dry ($SPEI3 = -1.44$). During the same period, the average temperature range, $T_{max} - T_{min}$, was $12.3\text{ }^{\circ}\text{C}$ in Ogulin, while it was only $7.5\text{ }^{\circ}\text{C}$ in Dubrovnik. Although the mean air temperature in Ogulin ($21.6\text{ }^{\circ}\text{C}$) was lower than the mean temperature in Dubrovnik ($27.8\text{ }^{\circ}\text{C}$), this resulted in a higher *PET* in Ogulin (475 mm) than in Dubrovnik (390 mm). Due to the higher precipitation, the three-month water

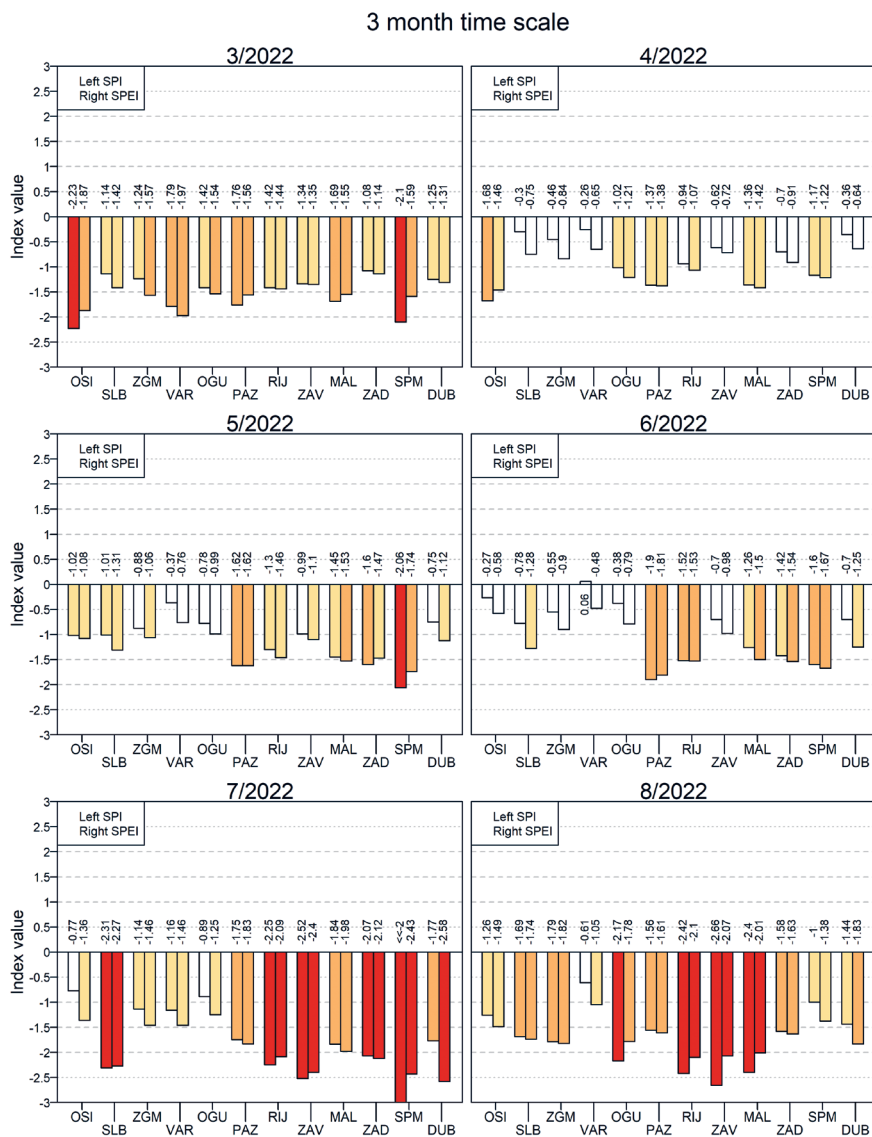


Figure 9. Comparison of *SPI* and *SPEI* on the 3-month scale from March to August 2022 for twelve stations in Croatia (marked with empty symbols in Fig. 1, running counterclockwise from the eastern mainland (Osijek-OSI) to the southern coastal of Croatia (Dubrovnik-DUB)).

balance in Ogulin was -320 mm ($SPEI_3 = -1.78$), while in Dubrovnik it was -346 mm ($SPEI_3 = -1.83$), so that both stations were classified as very dry by *SPEI*₃.

Figure 9 shows the three-month scale of *SPI* and *SPEI* values side by side for several stations across Croatia during the six months before the 2022 summer

drought. Dry conditions prevailed throughout the period shown. In general, it was moderately to severely dry until June, as the two indices show. The *SPEI* shows higher drought intensity in all but the most extreme cases, such as at stations OSI, PAZ and SPM. In July and August, drought severity increased significantly due to the cumulative dryness of the previous months. It is evident that the *SPI* almost always shows a higher intensity in extreme drought, as the main reason for extreme drought is the lack of precipitation. In other drought categories, the temperature effect is best seen via the *SPEI*, which increases the intensity of moderate drought and thus makes the spatial distribution of drought more uniform across all stations. When the intensity of the drought returns to normal, the *SPEI* lags behind the *SPI*, indicating prolonged duration of the drought. This can also serve as a precursor of an extreme drought in the following months if further precipitation deficits occur.

4. Discussion and conclusions

In this study, climatological drought monitoring with the *SPEI* index was analyzed with the primary goal of finding the best theoretical distribution for fitting the water balance (*P-PET*) in Croatia. The results aim to use the *SPEI* as an operational index for drought monitoring in Croatia in addition to the *SPI*. The *SPEI* has already been shown to account for the influence of temperature increase (Vicente-Serrano et al. 2010), but before it can be used operationally on a regional or country-wide scale, the best theoretical distribution for the local station data needs to be investigated. Monthly precipitation and air temperature values from 31 meteorological stations for the period 1961-2022 were used and the accumulations of *P-PET* were calculated for different time scales (1, 2, 3, 6, 9, 12, 18 and 24 months). The fitting was carried out using the method of L-moments. The ratio plots obtained (Figure 2) are in good agreement with the proposed regional classification. Among the five proposed distributions (with the respective pdf-s in Section 2), a three-parameter generalized logistic distribution (GLO) proved to be the most suitable, which also best represents the extreme events. The results thus confirmed the original recommendation made by Vicente-Serrano et al. (2010). There is a general agreement between *SPEI* and *SPI* time series, both in terms of sign and intensity. However, there was a tendency for higher drought intensity with *SPEI* compared to *SPI*, especially in the periods of light to moderate precipitation deficiency and high air temperature. Within these limitations, considerably higher absolute values for *SPEI* are observed in the continental region, where extreme temperatures are more pronounced during the summer months. As far as the historical series are concerned, quasi-periodic fluctuations between dry and wet periods were observed on larger time scales until the 1990s. Thereafter, the oscillation cycle shortened with more frequent extreme events, both wet and dry.

The changes toward increased severity of meteorological droughts can be associated with increased capacity of the atmosphere to absorb water vapor, which reduces surface humidity. (Vicente-Serrano et al., 2014). The results obtained are consistent with the consistent positive trends in surface air temperature reported by the IPCC (Masson-Delmotte et al., 2021).

As far as climate change in Croatia is concerned, there is a tendency towards drying out in warm seasons, especially along the Adriatic coast, and an increase in the frequency and severity of droughts can also be expected in the future (Gajić-Čapka et al., 2015; Ivušić et al., 2022). In addition, the coincidence of warm spells and drought in the Mediterranean (including the Adriatic) has increased, primarily due to temperature changes rather than lack of precipitation and has also extended beyond the warm season (Vogel et al., 2021). Similarly, the results of a recent 2022 summer drought study (Schumacher et al., 2023) indicate a long-term decline in summer soil moisture in the northern extratropics, likely fueled by regional warming.

In 2022, Croatia and many parts of Europe were hit by an extreme drought, which led to major economic losses in agriculture and caused record or near-record low water levels in many rivers (Toreti et al., 2022). A comparative analysis of the 2022 drought in Croatia confirmed that *SPEI* is able to detect a drought earlier than *SPI* and indicate a higher drought intensity due to large temperature anomalies. The drought in summer 2022 in Croatia was accompanied by several heat waves, leading to a kind of flash drought which could become a challenge for future drought management in a warming climate (Tijdeman et al., 2022) and has huge negative impacts. In the summer of 2022, 81% of the Croatian territory was affected by drought according to *SPI* (with normal conditions prevailing along the southern Adriatic) and 98% according to *SPEI*. The largest increase in spatial extent was found in the severely dry conditions class. These *SPEI* results are more in line with the effects of drought as reported in the media from agricultural fields in Croatia.

However, if we look at longer time scales, we see that the moderate to severe drought in Croatia lasted longer than 12 months, which led to drought in both agriculture (soil moisture deficit) and hydrology (low river flows and groundwater levels). The multi-year nature of the drought emphasises the need for continuous drought monitoring throughout the year (Tijdeman et al., 2022), as an earlier onset of heat and drought events can severely affect ecosystems and agriculture (Vogel et al., 2021).

Finally, in cases where there is a considerable precipitation deficit, especially if it accumulates over longer periods of time, drought monitoring can usually also be carried out using the *SPI*. Therefore, both indices are recommended in practice as they provide useful information for end users. The ODM in Croatia, complemented by the *SPEI*, will provide additional information to the public and stakeholders. It should be noted that more sophisticated methods of *PET* calculation, such as the Penman-Monteith equation, which requires a larger number

of variables in addition to precipitation and air temperature (e.g. relative humidity, surface pressure, wind speed, insolation), should enable even more realistic drought monitoring with the *SPEI*. This will be taken into account in the next upgrade of drought monitoring in Croatia.

References

- Allan, R. P., Hawkins, E., Bellouin, N. and Collins, B. (2021): IPCC, 2021: Summary for Policymakers, 32 pp, <https://doi.org/10.1017/9781009157896.001>
- Amatya, D. M., Skaggs, R. W. and Gregory, J. D. (1995): Comparison of methods for estimating REF-ET, *J. Irrig. Drain. Eng.*, **121**, 427–435, [https://doi.org/10.1061/\(ASCE\)0733-9437\(1995\)121:6\(427\)](https://doi.org/10.1061/(ASCE)0733-9437(1995)121:6(427)).
- Beguera, S., and Vicente-Serrano, S. M. (2022): Calculation of the Standardized Precipitation-Evapotranspiration Index R package, version 1.8.0, 21 pp. <https://doi.org/10.32614/CRAN.package.SPEI>
- Blain, G. C. (2014): Revisiting the critical values of the Lilliefors test: Towards the correct agrometeorological use of the Kolmogorov-Smirnov framework, *Bragantia*, **73**, 192–202, <https://doi.org/10.1590/brag.2014.015>.
- Blauhut, V., Stoezle, M., Ahopelto, L., Brunner, M. I., Teutschbein, C., Wendt, D. E., Akstinas, V., Bakke, S. J., Barker, L. J., Bartošová, L. et al. (2022): Lessons from the 2018–2019 European droughts: A collective need for unifying drought risk management, *Nat. Hazard. Earth Sys.*, **22**, 2201–2217, <https://doi.org/10.5194/nhess-22-2201-2022>.
- Cindrić, K., Juras, J. and Pasarić, Z. (2019): On precipitation monitoring with theoretical statistical distributions, *Theor. Appl. Climatol.*, **136**, 145–156, <https://doi.org/10.1007/s00704-018-2477-6>.
- Cindrić, K., Telišman Prtenjak, M., Herceg-Bulić, I., Mihajlović, D. and Pasarić, Z. (2016): Analysis of the extraordinary 2011/2012 drought in Croatia, *Theor. Appl. Climatol.*, **123**, 503–522, <https://doi.org/10.1007/s00704-014-1368-8>.
- Crutcher, H. L. (1975): A note on the possible misuse of the Kolmogorov-Smirnov test, *J. Appl. Meteorol.*, 1600–1603, [https://doi.org/10.1175/1520-0450\(1975\)014<1600:ANOTPM>2.0.CO;2](https://doi.org/10.1175/1520-0450(1975)014<1600:ANOTPM>2.0.CO;2).
- Droogers, P. and Allen, R. G. (2002): Estimating reference evapotranspiration under inaccurate data conditions, *Irrig. Drain. Sys.*, **16**, 33–45, <https://doi.org/10.1023/A:1015508322413>.
- Gajić-Čapka, M. and Zaninović, K. (1998): Secular variation of some water balance components at the Adriatic coast, *Proceedings Agriculture and Forestry – Adaptability to Climate Change*, Zagreb, Croatia, 19–20.
- Gajić-Čapka, M., Cindrić, K. and Pasarić, Z. (2015): Trends in precipitation indices in Croatia, 1961–2010, *Theor. Appl. Climatol.*, **121**, 167–177, <https://doi.org/10.1007/s00704-014-1217-9>.
- Hosking, J. R. M. (2022): L-Moments R package. <https://doi.org/10.32614/CRAN.package.lmom>
- Hosking, J. R. M. and Wallis, J. R. (1997): *Regional frequency analysis: An approach based on L-moments*. Cambridge University Press, UK, <http://dx.doi.org/10.1017/cbo9780511529443>.
- Ivušić, S., Güttler, I. and Horvath, K. (2022): Projected extreme precipitation changes over the coastal-mountainous region of the Eastern Adriatic and Dinaric Alps, *EMS Annual Meeting 2022*, Bonn, Germany, 5–9 September 2022, EMS2022-446, <https://doi.org/10.5194/ems2022-446>.
- Lloyd-Hughes, B. and Saunders, M. A. (2002): A drought climatology for Europe, *Int. J. Climatol.*, **22**, 1571–1592, <https://doi.org/10.1002/joc.846>.
- Masson-Delmotte, V., Zhai, P., Pirani, A., Connors, S. L., Péan, C., Berger, S., Caud, N., Chen, Y., Goldfarb, L., Gomis, M. I. et al. (2021): Climate Change 2021: The physical science basis, *Contribution of Working Group I to the Sixth Assessment Report of the Intergovernmental Panel on Climate Change*, **2**, 280 pp.
- McKee, T. B., Doesken, N. J. and Kleist, J. (1993): The relationship of drought frequency and duration to time scales, *Proceedings of the 8th Conference on Applied Climatology*, 17–22 January 1993, Anaheim, California, **17**, 179–183.

- Mihajlović, D. (2006): Monitoring the 2003–2004 meteorological drought over Pannonian part of Croatia, *Int. J. Climatol.*, **26**, 2213–2225, <https://doi.org/10.1002/joc.1366>.
- Pandžić, K. (1985): Water balance components on the Eastern Adriatic coastal region, *Rasprave-Papers*, **20**, 21–29 (In Croatian).
- Pandžić, K., Trninić, D., Likso, T. and Bošnjak, T. (2009): Long-term variations in water balance components for Croatia, *Theor. Appl. Climatol.*, **95**, 39–51, <https://doi.org/10.1007/s00704-007-0366-5>.
- Pandžić, K., Likso, T., Curić, O., Mesić, M., Pejić, I. and Pasarić, Z. (2020): Drought indices for the Zagreb-Grič Observatory with an overview of drought damage in agriculture in Croatia, *Theor. Appl. Climatol.*, **142**, 555–567, <https://doi.org/10.1007/s00704-020-03330-0>.
- Pandžić, K., Likso, T., Pejić, I., Šarčević, H., Pecina, M., Šestak, I., Tomšić, D. and Strelec Mahović, N. (2022): Application of the self-calibrated palmer drought severity index and standardized precipitation index for estimation of drought impact on maize grain yield in Pannonian part of Croatia, *Nat. Hazards*, **113**, 1237–1262, <https://doi.org/10.1007/s11069-022-05345-4>.
- Penzar, B. (1976): Drought indices for Zagreb and their statistical forecast, *Rasprave-Papers*, **13**, 1–58 (In Croatian).
- Schumacher, D. L., Zachariah, M., Otto, F., Barnes, C., Philip, S., Kew, S., Vahlberg, M., Singh, R., Heinrich, D., Arrighi, J. et al. (2023): Detecting the human fingerprint in the summer 2022 West-Central European soil drought, *EGUsphere*, **2023**, 1–41, <https://doi.org/10.5194/egusphere-2023-717>.
- Svoboda, M., Hayes, M. and Wood, D. (2012): *Standardized precipitation index: User guide*. WMO, Geneva, Switzerland, 16 pp.
- Syed, T. H., Famiglietti, J. S., Rodell, M., Chen, J. and Wilson, C. R. (2008): Analysis of terrestrial water storage changes from GRACE and GLDAS, *Water Resour. Res.*, **44**, <https://doi.org/10.1029/2006WR005779>.
- Tijdeman, E., Blauhut, V., Stoelzle, M., Menzel, L. and Stahl, K. (2022): Different drought types and the spatial variability in their hazard, impact, and propagation characteristics, *Nat. Hazard. Earth Sys.*, **22**, 2099–2116, <https://doi.org/10.5194/nhess-22-2099-2022>.
- Toreti, A., Bassu, S., Asseng, S., Zampieri, M., Ceglar, A. and Royo, C. (2022): Climate service driven adaptation may alleviate the impacts of climate change in agriculture, *Commun. Biol.*, **5**, 1–6, <https://doi.org/10.1038/s42003-022-04189-9>.
- Vicente-Serrano, S. M., Beguería, S. and López-Moreno, J. I. (2010): A multiscale drought index sensitive to global warming: The standardized precipitation evapotranspiration index, *J. Clim.*, **23**, 1696–1718, <https://doi.org/10.1175/2009JCLI2909.1>.
- Vicente-Serrano, S. M., Lopez-Moreno, J.-I., Beguería, S., Lorenzo-Lacruz, J., Sanchez-Lorenzo, A., García-Ruiz, J. M., Azorin-Molina, C., Morán-Tejeda, E., Revuelto, J., Trigo, R., Coelho, F. and Espejo, F. (2014): Evidence of increasing drought severity caused by temperature rise in southern Europe, *Environ. Res. Lett.*, **9**, 044001, <https://doi.org/10.1088/1748-9326/9/4/044001>.
- Vogel, J., Paton, E., Aich, V. and Bronstert, A. (2021): Increasing compound warm spells and droughts in the Mediterranean Basin, *Weather Clim. Ext.*, **32**, 100312, <https://doi.org/10.1016/j.wace.2021.100312>.
- Vučetić, M. and Vučetić, V. (1994): Evapotranspiration research in the Croatia lowlands, *Proceedings of Agriculture and Water Management*, 477–486.
- Vučetić, M., and Vučetić, V. (1996a): Evapotranspiration in the mountain area of Croatia, *Proceedings of the 24th International Conference on Alpine Meteorology*, Bled, Slovenia, 9–13 September 1996, 401–408.
- Vučetić, M., and Vučetić, V. (1996b): Determination of evapotranspiration in Croatia, in *Biometeorology*, **14**, 141–148.
- Wilks, D. S. (2011): *Statistical methods in the atmospheric sciences*. Academic Press., 704 pp.
- Zargar, A., Sadiq, R., Naser, B. and Khan, F. I. (2011): A review of drought indices, *Environ. Rev.*, **19**, 333–349, <https://doi.org/10.1139/a11-013>.

SAŽETAK

Praćenje suše u Hrvatskoj standardiziranim oborinsko evapotranspiracijskim indeksom*Ivan Lončar-Petrinjak, Zoran Pasarić i Ksenija Cindrić Kalin*

Nekoliko suša tijekom posljednjeg stoljeća teško su pogodile velike dijelove Europe uzrokujući velike ekonomske gubitke, posebno u poljoprivrednom i energetskom sektoru. Iako je manjak oborine glavni pokretač suše, visoke temperature ljetnih mjeseci dodatno pojačavaju njen intenzitet s potencijalno razornim posljedicama. Takav slučaj dogodio se 2022. godine kada su se za vrijeme dugih sušnih razdoblja pojavili i toplinski valovi. U ovom radu, analizirana je primjena Standardiziranog oborinsko evapotranspiracijskog indeksa (*SPEI*) u klimatološkom monitoringu s glavnim ciljem određivanja najbolje teorijske razdiobe za opis vodne bilance (definirane kao razlika između oborine i potencijalne evapotranspiracije) u Hrvatskoj. Ovo je potrebno učiniti prije uvođenja samog indeksa u operativni monitoring suše. Iako se *SPEI* često koristi za monitoring suše, taj indeks koristi razdiobu vodne bilance koja može bitno varirati ovisno o lokaciji. Ovo istraživanje temeljeno je na mjesečnim vrijednostima količine oborine i srednjim mjesečnim minimalnim i maksimalnim dnevnim temperaturama zraka zabilježenih na 31 glavnoj meteorološkoj postaji u periodu od 1961. do 2022. Analiza je provedena za više vremenskih skala u rasponu od 1 do 24 mjeseca. Razmotreno je pet teorijskih razdioba od kojih se tropometarska generalizirana logistička (*GLO*) razdioba pokazala kao najprikladnija. Pokazano je da postoji generalno poklapanje vremenskih nizova indeksa *SPI* i *SPEI* u predznaku i intenzitetu. Primjetna je tendencija da *SPEI* pokazuje veću sušnost u umjerenom sušnim i vrlo sušnim ali vrućim razdobljima. Usporedna analiza suše ljeta 2022. potvrđuje mogućnost *SPEI* da detektira sušu ranije od *SPI* u okolnostima kada temperature zraka bitno odstupaju od uobičajenih vrijednosti.

Ključne riječi: suša, oborina, temperatura zraka, *SPI*, *SPEI*, generalizirana logistička razdioba, L-momenti

Corresponding author's address: Ivan Lončar-Petrinjak, Croatian Meteorological and Hydrological Service, Ravnice 48, 10000 Zagreb, Croatia; tel.: +385 1 4565 738; e-mail: ilpetrinjak@cirus.dhz.hr



This work is licensed under a Creative Commons Attribution-NonCommercial 4.0 International License.